Front. Optoelectron. 2012, 5(1): 94–98
DOI 10.1007/s12200-012-0190-0

RESEARCH ARTICLE

Design of unidirectional emission silicon/III-V laser for on-chip interconnects

Chucai GUO[1,2], Yongzhen HUANG (✉)[1], Yuede YANG[1], Xiaomeng LV[1], Qifeng YAO[1]

1 State Key Laboratory on Integrated Optoelectronics, Institute of Semiconductors, Chinese Academy of Sciences, Beijing 100083, China
2 College of Optoelectronic Science and Engineering, National University of Defense Technology, Changsha 410073, China

Abstract We propose a unidirectional emission silicon/III-V laser, which comprises an III-V quantum wells microdisk connected to an output waveguide and a silicon-on-insulator (SOI) waveguide. Characteristics of the III-V microdisk with an output waveguide and mode coupling between the III-V output waveguide and the SOI waveguide are investigated by three-dimensional (3D) finite-difference time-domain (FDTD) method. Simulation results show that the Q factor of a coupled mode for a 7.5 μm diameter microdisk connected to a 0.5 μm wide output waveguide is about 8.5×10^4. And the coupling efficiency between the III-V output waveguide and the SOI waveguide is over 96% when the III-V waveguide width is 0.5 μm, the SOI waveguide width is 0.565 μm and the vertical gap between those two waveguides is 0.1 μm. The proposed hybrid laser would be of valuable applications for on-chip interconnects.

Keywords silicon/III-V laser, unidirectional emission, three-dimensional (3D) finite-difference time-domain (FDTD) method, on-chip interconnects

1 Introduction

Nowadays, on-chip optical interconnects have drawn a great research attentions for their valuable advantages over electrical interconnects, such as wide bandwidth and low-power consumption. Silicon photonics is widely considered as a promising platform for realizing on-chip optical interconnects. Recent advances in silicon photonics, such as low loss waveguides [1], narrowband filters [2], optical demultiplexer [3], fast modulators [4] and Ge-on-Si photodetectors [5], have been already demonstrated. However, bulk silicon has very low efficiency of light emission due to its indirect bandgap. Therefore, achieving practical laser sources has been one of most challenging goals in silicon photonics.

In order to realize efficient silicon based laser sources, silicon/III-V hybrid lasers have been recently demonstrated, including III-V microdisk lasers [6,7] and microring lasers [8] vertically coupled to a silicon-on-insulator (SOI) bus-waveguide. One shortcoming of the demonstrated hybrid lasers is the bi-directional laser emissions, which imposes additional structures in order to re-route or combine the laser emissions.

Recently, we have proposed and demonstrated III-V microdisk lasers with an output waveguide for realizing unidirectional emission laser sources [9,10]. And in this study, we propose a new silicon/III-V laser structure, where an III-V microdisk connected with an output waveguide is used to provide the gain and then the laser emission in the III-V output waveguide is vertically coupled to a SOI waveguide. The proposed unidirectional emission hybrid laser would be more compact and more favorable for on-chip optical interconnects.

2 Simulation and analysis

Layout of the proposed unidirectional silicon/III-V hybrid laser is shown in Fig. 1. The proposed laser comprises mainly two parts, one part is an III-V microdisk connected directly to an output waveguide, and the other part is an SOI waveguide. And two parts of the hybrid laser are integrated together through benzocyclobutene (BCB) bonding [11]. For the III-V microdisk structure, it comprises a gain material (quantum wells) layer sandwiched between two layers of InP. The thickness of the gain material layer and the upper InP layer are t_g and t_u, respectively. The bottom InP layer is etched incompletely, leaving a thin lateral bottom contact layer with thickness t_l, and the thickness of the etched bottom InP layer is t_b. The

Received August 29, 2011; accepted September 14, 2011

E-mail: yzhuang@semi.ac.cn

III-V microdisk has a diameter D and the output waveguide has a width w_1. For the SOI waveguide, it has a width w_2 and a height h. The III-V output waveguide is laterally aligned to the SOI waveguide, and the III-V microdisk with the output waveguide is embedded in a thick BCB layer which is not drawn on Fig. 1.

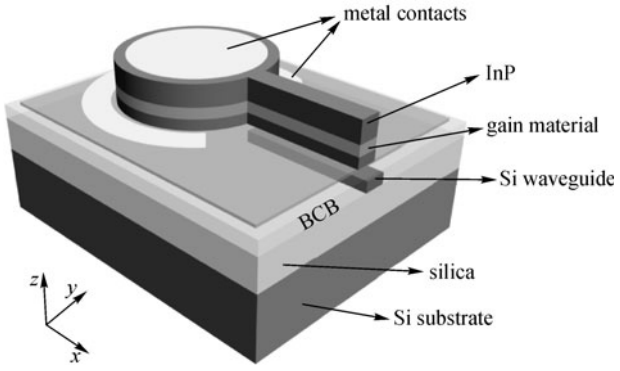

Fig. 1 Schematic figure of unidirectional silicon/III-V hybrid laser

In the following, the characteristics of the III-V microdisk with an output waveguide and the mode coupling between the III-V output waveguide and the SOI waveguide are respectively investigated by using three-dimensional (3D) finite-difference time-domain (FDTD) method.

When a microdisk is connected to an output waveguide, the output waveguide will destroy the symmetry of the microdisk and result in the mode coupling of two whispering gallery modes (WGMs) in the corresponding perfect microdisk [9,12]. If a coupled mode corresponds to two high-Q modes in a perfect microdisk with very small wavelength difference, the Q factor of the coupled mode can be very high. Figure 2 shows the intensity spectrum for a microdisk with an output waveguide, which is obtained by FDTD simulation and Padé approximation [13]. The intensity spectrum is calculated from the time transience of the H_z component recorded at an arbitrarily selected point inside the microdisk. By fitting the peaks of the intensity spectrum with Lorentzian functions, we can obtain the mode frequency and Q factor from the peak frequency and the ratio of the peak frequency to the corresponding 3 dB bandwidth. As is shown in Fig. 2, there are three modes in the calculated wavelength range, which are denoted as modes A, B and C, respectively. Simulation results show that the Q factors of the three modes are 8.5×10^4, 1.5×10^4 and 6.4×10^3, and the corresponding mode wavelength are 1525.8, 1556.2 and 1587.6 nm, respectively. Parameters used in the simulation are as follows, refractive index of BCB $n_{\mathrm{BCB}} = 1.54$, refractive index of gain material $n_{\mathrm{g}} = 3.40$, refractive index of InP $n_{\mathrm{InP}} = 3.17$, $D = 7.5$ μm, $w_1 = 500$ nm, $t_{\mathrm{g}} = 300$ nm, $t_{\mathrm{u}} = 150$ nm, $t_{\mathrm{b}} = 100$ nm, $t_{\mathrm{l}} = 50$ nm. The three modes in Fig. 2 are all coupled modes, and each of them is formed by coupling of two resonant modes in a corresponding perfect microdisk without an output waveguide. Figures 3(a)–3(c) show the two resonant modes in the perfect microdisk, which are related to modes A, B and C in Fig. 2, respectively. The differences of wavelength between the two resonant modes in Figs. 3(a)–3(c) are 0.2, 1.8 and 3.3 nm, respectively. Because the two resonant modes corresponding to mode A have the smallest wavelength difference, the Q factor of mode A is the

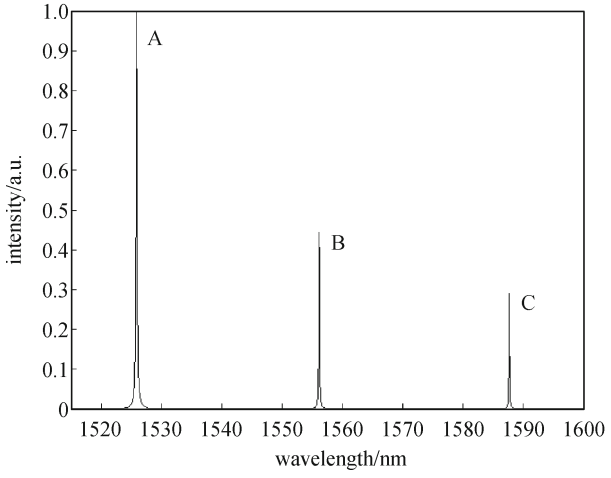

Fig. 2 Intensity spectrum for microdisk with output waveguide obtained by FDTD simulation and Padé approximation

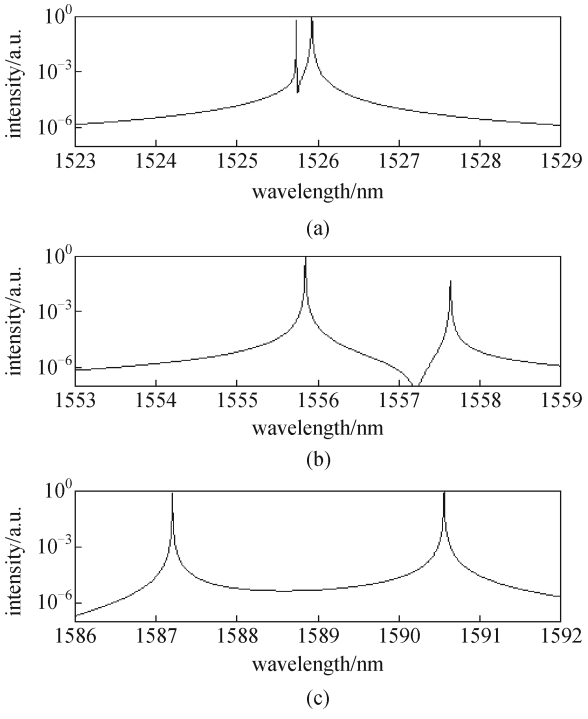

Fig. 3 Intensity spectra for perfect microdisk without output waveguide. Two resonant modes correspond to modes (a) A; (b) B; (c) C in Fig. 2

highest among that of those three modes in Fig. 2. Figures 4(a) and 4(b) show the magnetic filed component H_z distribution of mode A in Fig. 2 at the center plane of the gain material layer and at x-O-z plane respectively, the field in the output waveguide is magnified 30 times. As is shown in Fig. 4, most field of this mode is well confined in the gain material layer of the microdisk.

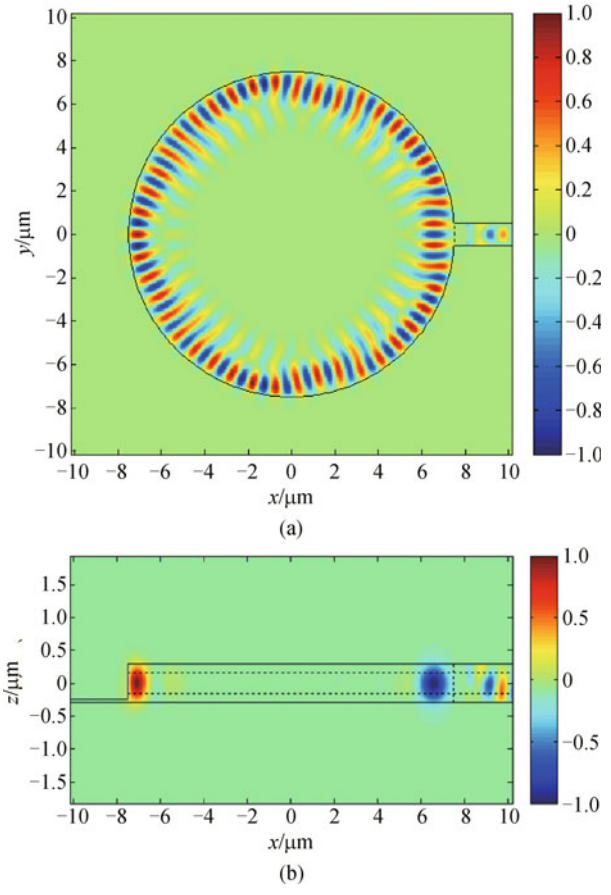

Fig. 4 Magnetic field component H_z distribution of mode A in Fig. 2 at (a) center plane of gain material layer; (b) x-O-z plane. Field in output waveguide is magnified 30 times

As for the mode coupling between the III-V output waveguide and the SOI waveguide, if we choose a proper size of the SOI waveguide after determining the size of III-V waveguide, the coupling efficiency between those two waveguides can be close to 100%. Figure 5 shows the effective index of the fundament mode as a function of the mode wavelength for an III-V waveguide and three SOI waveguides with different widths. Parameters of the III-V waveguide in Fig. 5 are the same as that in Fig. 2. And parameters of the SOI waveguide other than the width used in Fig. 5 are as follows, h = 340 nm, refractive index of silicon n_{Si} = 3.48 and refractive index of the buried oxide layer of SOI n_{SiO_2} = 1.45. As is shown in Fig. 5, when w_2 = 565 nm, the modes of the III-V waveguide and the SOI waveguide have almost the same effective index N around the wavelength of 1525.8 nm (resonant wavelength of mode A in Fig. 2). The dispersion curves in Fig. 5 are calculated by 3D FDTD method with periodic boundary condition [14] in x direction. Figures 6(a) and 6(b) show the magnetic filed component H_z distributions of the fundament mode at the cross section (y-O-z plane) of the III-V waveguide and SOI waveguide with w_2 = 565 nm, other parameters used in Fig. 6 are the same as in Fig. 5.

When an III-V waveguide is put on top of a SOI waveguide, the guided mode in the III-V waveguide can be coupled efficiently to the SOI waveguide if those two waveguides have similar effective index. Figure 7(a) shows the steady-state distribution of H_z at x-O-z plane of the coupled III-V waveguide and SOI waveguide. Figures 7(b) and 7(c) show the H_z distributions at the center plane of III-V waveguide and SOI waveguide, respectively. A Gaussian beam at wavelength of 1525.8 nm is injected from the left port of the III-V waveguide in Fig. 7, and the light is coupled from the III-V waveguide to

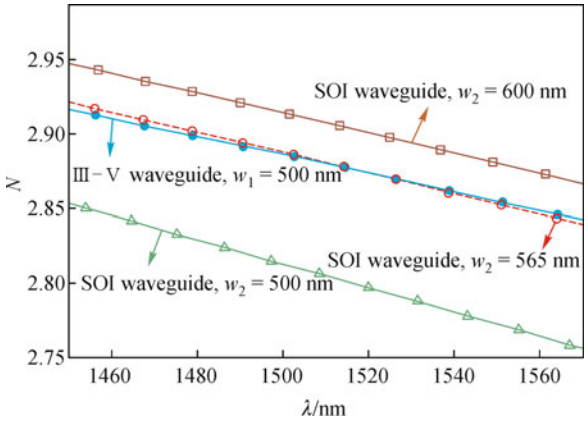

Fig. 5 Effective index of fundament mode as function of mode wavelength for III-V waveguide and three SOI waveguides with different widths

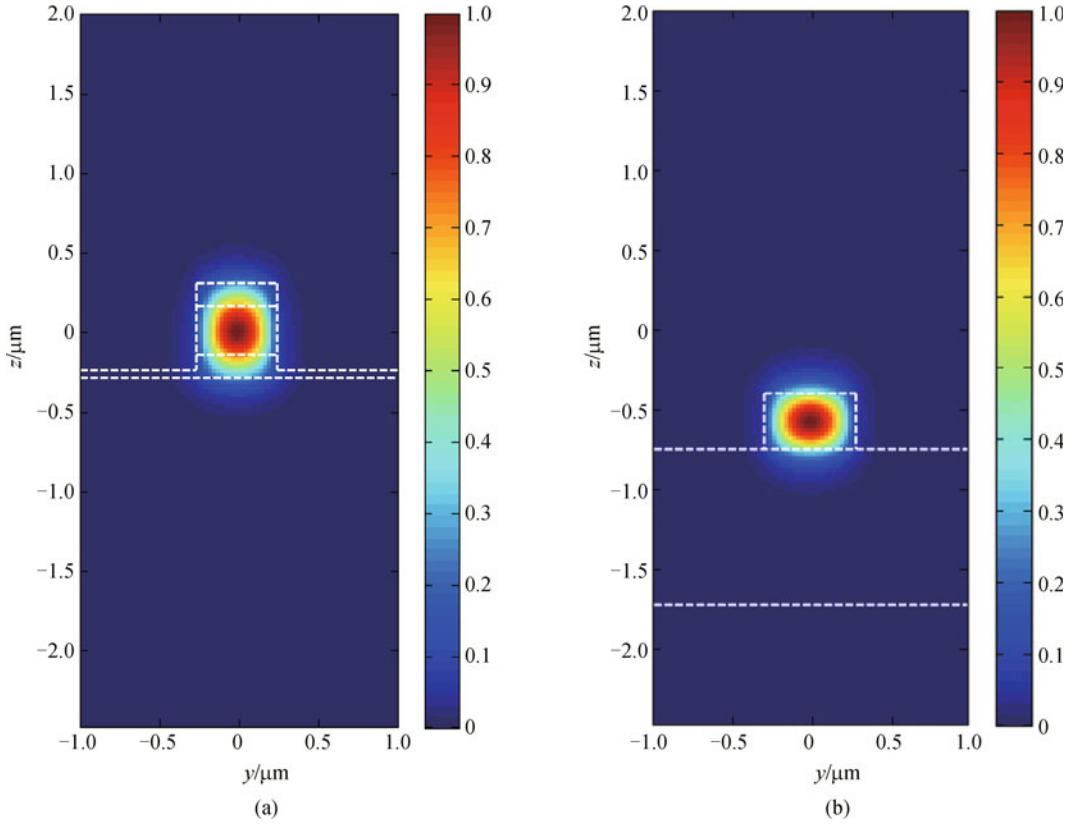

Fig. 6 H_z distribution of fundament mode at the cross section of (a) III-V waveguide and (b) SOI waveguide with w_2 = 565 nm

the underlying SOI waveguide in the coupling region. After the coupling region, the light is guided by the SOI waveguide. Waveguide parameters used in Fig. 7 are the same as that in Fig. 6, and the BCB thickness between the III-V waveguide and the SOI waveguide is 100 nm, and the length of the coupling region is 9.4 μm. Simulation result shows that coupling efficiency, which is defined as the ratio of the energy flux confined in the SOI waveguide after the

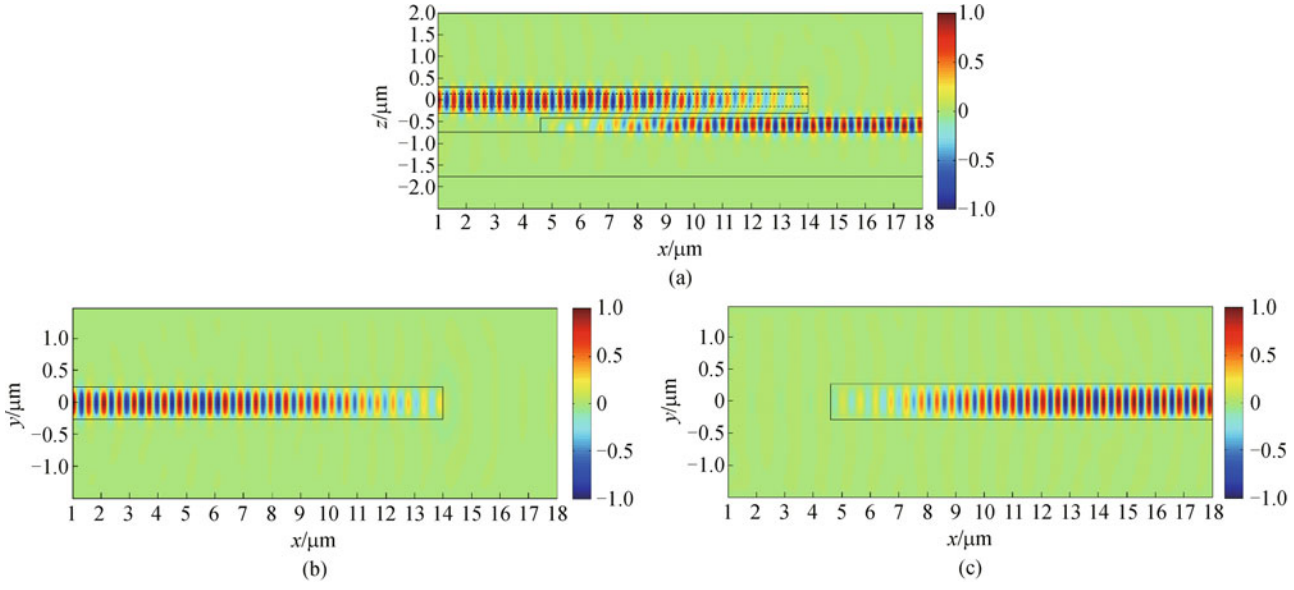

Fig. 7 Steady-state distribution of H_z at (a) *x*-*O*-*z* plane of coupled waveguides; (b) center plane of III-V waveguide; and (c) center plane of SOI waveguide

coupling region to the energy flux confined in the III-V waveguide before the coupling region, is over 96%. If the effective indexes of the III-V waveguide and the SOI waveguide are mismatched, the coupling efficiency will decrease. For example, if we choose w_2 = 500 nm, the highest coupling efficiency of those two waveguides will decrease to 73%.

3 Conclusions

We proposed a unidirectional emission silicon/III-V hybrid laser by using BCB bonding of an III-V quantum wells microdisk with an output waveguide on top of a SOI waveguide. A high Q mode in the microdisk with an output waveguide and high coupling efficiency between the III-V waveguide and SOI waveguide have been identified by 3D FDTD simulations. The proposed hybrid laser would be of useful application in on-chip interconnects for its uni-port emission, small size, high quality factor and high coupling efficiency.

References

1. Vlasov Y A, McNab S J. Losses in single-mode silicon-on-insulator strip waveguides and bends. Optics Express, 2004, 12(8): 1622–1631
2. Takano H, Song B S, Asano T, Noda S. Highly efficient multi-channel drop filter in a two-dimensional hetero photonic crystal. Optics Express, 2006, 14(8): 3491–3496
3. Brouckaert J, Bogaerts W, Dumon P, Van Thourhout D, Baets R. Planar concave grating demultiplexer fabricated on a nanophotonic silicon-on-insulator platform. Journal of Lightwave Technology, 2007, 25(5): 1269–1275
4. Xu Q F, Manipatruni S, Schmidt B, Shakya J, Lipson M. 12.5 Gbit/s carrier-injection-based silicon micro-ring silicon modulators. Optics Express, 2007, 15(2): 430–436
5. Michel J, Liu J F, Kimerling L C. High-performance Ge-on-Si photodetectors. Nature Photonics, 2010, 4(8): 527–534
6. van Campenhout J, Rojo Romeo P, Regreny P, Seassal C, van Thourhout D, Verstuyft S, Di Cioccio L, Fedeli J M, Lagahe C, Baets R. Electrically pumped InP-based microdisk lasers integrated with a nanophotonic silicon-on-insulator waveguide circuit. Optics Express, 2007, 15(11): 6744–6749
7. van Campenhout J, Liu L, Romeo P R, van Thourhout D, Seassal C, Regreny P, Di Cioccio L, Fedeli J M, Baets R. A compact SOI-integrated multiwavelength laser source based on cascaded InP microdisks. IEEE Photonics Technology Letters, 2008, 20(16): 1345–1347
8. Liang D, Fiorentino M, Okumura T, Chang H H, Spencer D T, Kuo Y H, Fang A W, Dai D, Beausoleil R G, Bowers J E. Electrically-pumped compact hybrid silicon microring lasers for optical interconnects. Optics Express, 2009, 17(22): 20355–20364
9. Yang Y D, Wang S J, Huang Y Z. Investigation of mode coupling in a microdisk resonator for realizing directional emission. Optics Express, 2009, 17(25): 23010–23015
10. Wang S J, Lin J D, Huang Y Z, Yang Y D, Che K J, Xiao J L, Du Y, Fan Z C. AlGaInAs/InP microcylinder lasers connected with an output waveguide. IEEE Photonics Technology Letters, 2010, 22 (18): 1349–1351
11. Roelkens G, Van Thourhout D, Baets R. Ultra-thin benzocyclobutene bonding of III–V dies onto SOI substrates. Electronics Letters, 2005, 41(9): 561–562
12. Guo C C, Huang Y Z. Mode analysis for in-plane emission microdisk resonator. In: Proceedings of SOPO'2011. 2011, 1–3
13. Guo W H, Li W J, Huang Y Z. Computation of resonator frequencies and quality factors of cavities by FDTD technique and Padé approximation. IEEE Microwave and Wireless Components Letters, 2001, 11(5): 223–225
14. Chutinan A, Noda S. Waveguides and waveguide bends in two-dimensional photonic crystal slabs. Physical Review B: Condensed Matter and Materials Physics, 2000, 62(7): 4488–4492